

# Ice and Water Permittivities for Millimeter and Sub-millimeter Remote Sensing Applications

Jonathan H. Jiang and Dong L. Wu

Jet Propulsion Laboratory, California Institute of Technology, Pasadena, California

## Abstract

Recent advances of satellite remote sensing at near-millimeter and sub-millimeter wavelengths ( $\sim 100$ - $3000$  GHz) require accurate complex permittivity for ice and liquid water at these frequencies for different temperatures, especially for cold atmospheric conditions. This paper summarizes the existing experimental permittivity data in the previous literature, and provides an updated empirical permittivity model for radiative transfer calculations for ground and space applications. Applications of this permittivity model to Microwave Limb Sounder (MLS) cloud measurements are discussed.

## 1. Introduction

Modeling cloud radiative properties requires knowledge of the relative refractive index  $m = m_1/m_o$  of ice and water hydrometers, where  $m_1 = n' - in''$  is a complex refractive number and  $m_o$  is the index of the surrounding medium. For the Earth's atmosphere,  $m_o = 1$ , and  $m$  is simply equal to the particle refractive index, which is the square root of the complex dielectric permittivity  $\epsilon$ ,

$$m = \sqrt{\epsilon} \quad (1)$$

where 
$$\epsilon = \epsilon' - i\epsilon'' \quad (2)$$

The real part of the permittivity,  $\epsilon'$ , or dielectric constant, is a parameter describing how electromagnetic fields are stored; the imaginary part,  $\epsilon''$ , or loss factor, describes how electromagnetic fields are absorbed.

The dielectric properties ( $\epsilon'$ ,  $\epsilon''$ ) of ice and water plays a key role in computing radiative transfer propagation and effects caused by ice and water hydrometers suspended in clouds. For MLS (Microwave Limb Sounder) cloud measurements, we developed an empirical model based on the original parameterizations in *Liebe et al.* [1989, 1991] and *Hufford* [1991] (hereafter LH model). The LH model was developed mainly from experimental data at frequencies  $< 1000$  GHz for both ice and water, and limited to temperatures  $\geq 0^\circ\text{C}$  for water. The Earth Observing System (EOS) MLS experiment (due for launch in June 2004), requires knowledge of the dielectric properties of ice and water at frequencies upto 2500 GHz and at super-cold temperatures. Because of limited experimental data in developing the original LH model, especially for the imaginary part of the permittivity of ice at high frequencies (600-2500 GHz), some uncertainty may affect calculations of ice cloud remote sensing effects with this LH model.

In this paper, we extend the LH dielectric permittivity ( $\epsilon'$ ,  $\epsilon''$ ) model for pure ice to frequencies upto 4000 GHz and update the parameterization by comparing of the modeled ice

and water permittivity to laboratory measurements reported in the literature. Applications to the Mie calculations and uncertainties at EOS MLS frequencies are discussed.

## 2. The complex permittivity for pure ice and water at 1-2500 GHz

For pure-water ice, the LH model formulates the complex permittivity by

$$\begin{aligned}\epsilon'_{ice} &= 3.15 \\ \epsilon''_{ice} &= \alpha(T)/\nu + \beta(T)\nu\end{aligned}\quad (3)$$

where  $\nu$  is frequency in GHz, and  $\alpha(T)$  and  $\beta(T)$  are temperature dependent parameters fitted to laboratory measurements [Hufford, 1991]. For pure liquid water, the formulations are:

$$\begin{aligned}\epsilon'_{water} &= (\epsilon_0 - 5.48)/[1 + (\nu/\nu_p)^2] + 1.97/[1 + (\nu/\nu_s)^2] + 3.51 \\ \epsilon''_{water} &= (\epsilon_0 - 5.48)(\nu/\nu_p)/[1 + (\nu/\nu_p)^2] + 1.97(\nu/\nu_p)/[1 + (\nu/\nu_p)^2]\end{aligned}\quad (4)$$

where  $\epsilon_0$ ,  $\nu_p$  and  $\nu_s$  are all temperature dependent parameters [Liebe *et al.*, 1991].

To extend the LH formulae to frequencies  $>1000$  GHz, we modified the LH expression for imaginary part of the dielectric permittivity of ice by including a  $\nu^3$  term in Equation (3), based on the far-infrared work by *Mishima et al.* [1983], namely

$$\epsilon''_{ice} = \alpha(T)/\nu + \beta(T)\nu + \gamma\nu^3 \quad (5)$$

where  $\gamma = 1.16 \times 10^{-11}$  as calculated from the  $B$  factor in Eqn-16 in *Mishima et al.* [1983]. For the real part of the ice permittivity, we assume the LH formula stays the same at higher frequencies, as do the real and imaginary parts of permittivity of water.

## 3. Comparisons to laboratory measurements

### 3.1 The permittivity of pure ice

Laboratory measurements of the imaginary part of the ice refractive index or dielectric permittivity have been made and published by a number of researchers at millimeter and sub-millimeter wavelengths, and they are summarized in Figure 1 with comparison to the modified LH model (Equation 5). The solid lines in Figure 1 show the imaginary ice dielectric permittivity computed by the modified LH model at different temperatures. The dotted-lines are the original curves computed from the original LH formula (Equation 3). The measured data are described in the following.

*Matzler and Wegmuller* [1987] presented measurements for coefficient  $\beta$  (of the Equation 3) at temperatures between 0 and  $-30^\circ\text{C}$ . The values of their  $\epsilon''$  at  $-3^\circ\text{C}$  and  $-10^\circ\text{C}$  are estimated by using the modified LH formula. *Perry and Straiton* [1973] obtained values of  $\epsilon'$  and  $\epsilon''$  from measurements at  $-28^\circ\text{C}$ . *Mishima, Klug and Whalley* [1983] measured the absorption spectrum from  $8\text{-}25\text{ cm}^{-1}$  ( $400\text{-}1250\text{ }\mu\text{m}$  wavelength or  $240\text{-}750$  GHz) for single crystals of ice at four temperatures (80, 100, 150, 202 K). The plotted values of imaginary dielectric constant  $\epsilon''$  are estimated from their measurements of  $n''$  at 202 K and assuming  $\epsilon' = 3.15$ . *Whalley and Labbe* [1969] measured the absorption spectrum from  $17\text{-}42\text{ cm}^{-1}$  ( $238\text{-}588\text{ }\mu\text{m}$  wavelength or  $510\text{-}1260$  GHz) for blocks of ice at 100 and 200 K. We converted their measured values of  $n''$  to  $\epsilon''$  also assuming  $\epsilon' = 3.15$ . *Berte, Labbe and Whalley* [1969] made measurements for thin

films of ice ( $< 1 \mu\text{m}$  thick) at 100 K from  $100\text{-}8000 \text{ cm}^{-1}$  (or  $3000\text{GHz}$  to  $240 \text{ THz}$ ). The plotted  $\epsilon''$  are taken from their table III. They also presented some “preliminary and not very accurate” measurements of a  $1\text{-mm}$  thick sample for  $30\text{-}60 \text{ cm}^{-1}$  ( $900\text{-}1800 \text{ GHz}$ ) and estimated value at  $80 \text{ cm}^{-1}$  ( $2400 \text{ GHz}$ ).

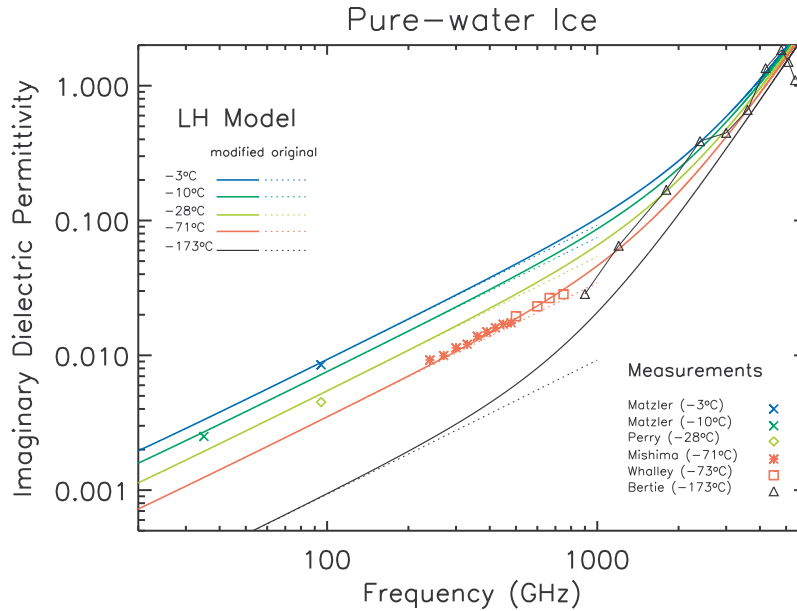


**Figure 1:** Computed and measured imaginary part of ice dielectric permittivities. The solid-lines are  $\epsilon''$  computed using the modified LH formula (6), the dotted-lines those computed using the original LH formula (3).

In the comparisons with the laboratory data, we found the differences between the modified LH model results and the measurements is generally less than  $\sim 12\%$  for frequencies  $< 800 \text{ GHz}$  and about  $15\text{-}40\%$  at frequencies  $\geq 3000 \text{ GHz}$ . In the frequency range of  $900\text{-}2400 \text{ GHz}$ , the only available data are the preliminary measurements by *Berte, Labbe and Whalley* [1969], which may have large errors as stated in their paper.

The measured values for the real part of ice permittivity  $\epsilon'$  are shown on Figure 2. The data labeled ‘from Ulaby’ are taken from *Ulaby, Moore and Fung* [1981], which consisted a set of measurements by *Cumming* [1952], *Hippel* [1954], *Vant et al.* [1974], *Lamb* [1946], *Lamb and Turney* 1949, *Perry and Straiton* 1973. Other data are from *Bertie et al.* 1969.

The measured real permittivities of ice remain fairly constant over the broad microwave spectrum. Differences between the various measured data and the LH model value of 3.15 (shown as the straight line in Figure 2) are generally less than  $5\%$  at frequencies  $< 1000 \text{ GHz}$ . At higher frequencies ( $> 1000 \text{ GHz}$ ) the differences increase slightly but remain  $< 15\%$  in general.

### 3.2 The permittivity for pure liquid water

For liquid water, the measured real and imaginary parts of dielectric permittivity are shown in Figure 2 and Figure 3, respectively. Measurements by *Lowan* [1949], *Klein and Swift* [1977] were at frequencies mainly below  $120 \text{ GHz}$ , while the data from *Liebe et al.* [1991] are in the range from  $5\text{-}410 \text{ GHz}$  for temperatures  $\leq 20^\circ\text{C}$ .

The differences between measurements and the LH model as shown in Figures 2 and 3 are generally less than  $\sim 5\%$ . However, few measurements are made below  $0^\circ\text{C}$ . Values of the dielectric permittivity of super-cold pure liquid water ( $< 0^\circ\text{C}$ ) are mostly computed from models [e.g. *Ulaby et al.* 1981, (p2020-2025); *Hulst* 1981, (p281-284)].

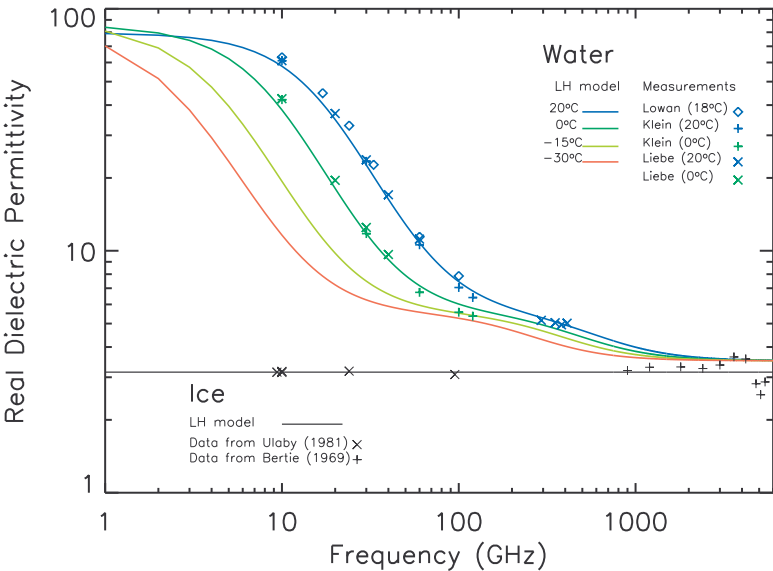


**Figure 2:** Computed and measured real part of ice and water dielectric permittivities. The solid curves are  $\epsilon'$  computed using the modified LH formula (3) for ice and (4) for liquid water.

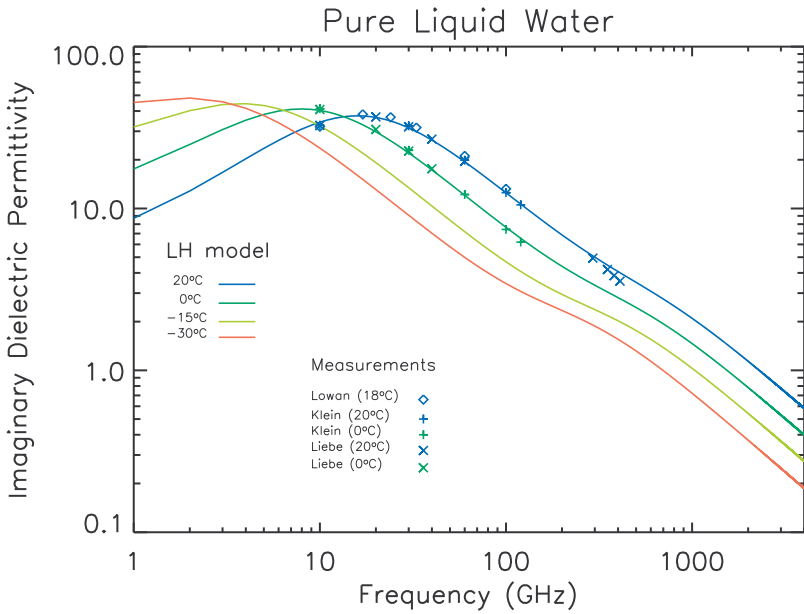


**Figure 3:** Computed and measured imaginary part of liquid water dielectric permittivities. The solid curves are  $\epsilon''$  computed using the modified LH formula (4).

#### 4. Sensitivity in microwave remote sensing applications

Cloud measurements using passive microwave instruments from space are relatively new and have important atmospheric applications. For example, recent observations with the limb-viewing MLS instrument on board the Upper Atmosphere Research Satellite (UARS) to obtain cloud occurrence frequency and cloud ice content information for thick ice clouds in the upper troposphere has shown important applications in research related to the convective scale perturbations in the tropical tropopause layer (TTL) and their potential influence on stratospheric dehydration [e.g. *Jiang et al.*, 2004, *Read et al.*, 2004; *Wu et al.* 2004].

Ice particles and water droplets have different Mie radiative properties in these cold air conditions, mainly caused by their permittivity differences. Figure 4a shows the Mie extinction (solid-lines) and scattering (dotted-lines) efficiencies calculated at 4 selected MLS frequencies for ice particles (blue) and water droplets (red) at diameters between 1-4000 microns. The complex permittivities for ice and liquid water are computed for typical mid- to upper-tropospheric temperatures of  $-60^{\circ}\text{C}$  and  $-15^{\circ}\text{C}$ , respectively. From this example we see that the Mie extinction and scattering efficiencies of small liquid water particles (diameter  $< 500 \mu\text{m}$ ) are much higher than those of small ice particles. Most importantly, for these ice particles, which account for most cloud ice contents in the upper-troposphere, scattering occurs nearly in the Rayleigh regime at the MLS frequencies. In other words, for most upper-tropospheric clouds, the Mie coefficient increases with ice particle size.

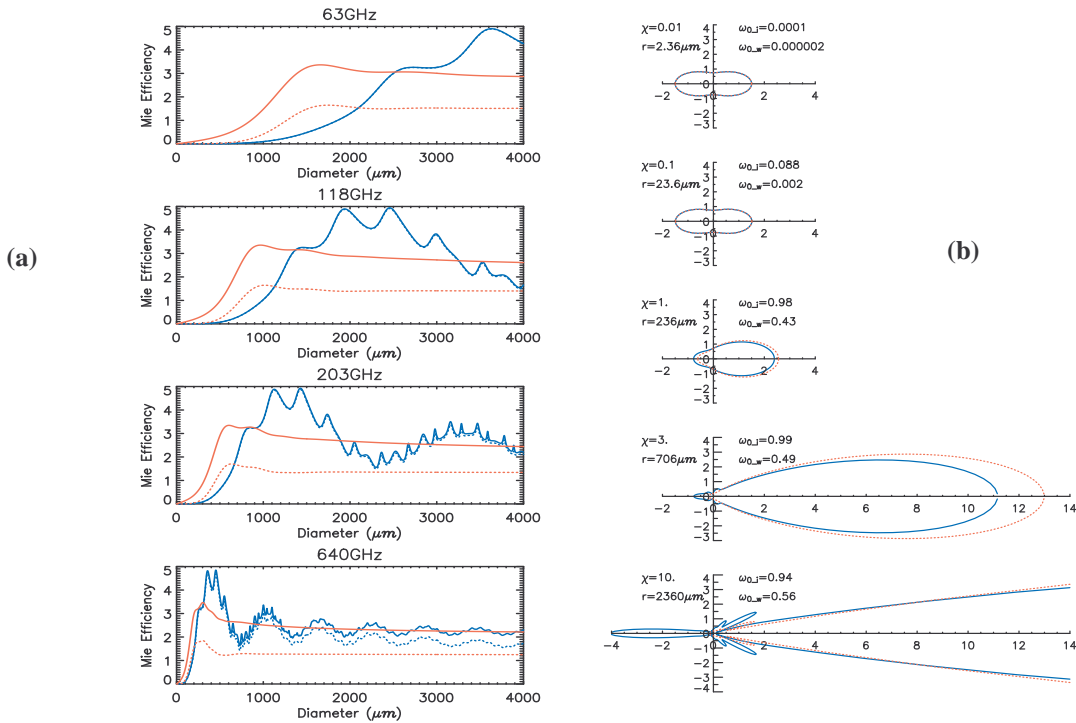


**Figure 4:** (a) Mie extinction (solid-line) and scattering (dotted-line) efficiencies for ice (blue) and liquid water (red); (b) Phase function for single ice particles (solid-line) and water droplet (dotted-line) with different size parameters. The complex dielectric permittivities are computed at  $-60^{\circ}\text{C}$  for ice and  $-15^{\circ}\text{C}$  for liquid water.

The Mie phase function depends mainly upon the particle size parameter ( $\chi = 2\pi r/\lambda$ ), but it is also influenced by the complex permittivity. Figure 4b illustrates the computed phase functions for single ice particles and water droplets with various particle size parameters. The

dielectric permittivity values are computed for ice or water at 203GHz using the same temperatures as in Figure 4a. The single scattering albedo ( $\omega_0$ ) shown for each particle size is the ratio of Mie scattering to extinction efficiencies. For small size parameter (e.g.  $\chi < 0.1$ ), both the ice and water scatter radiation in nearly equal quantities forwards and backwards, the single scattering albedo is small. For large size parameter (e.g.  $\chi > 1$ ), the radiation is heavily concentrated in a narrow forward lobe, the single scattering albedo increases, and the ice and water phase functions become different. At very large size parameter (e.g.  $\chi = 10$ ), the backward scattering of ice particles is much larger than that of liquid droplets. Also notably, the single scattering albedo of ice ( $\omega_{0,i}$ ) is much larger than that of water ( $\omega_{0,w}$ ) for all particle sizes, mainly due to the difference in Mie efficiencies.

In practice, we have found ice particles with diameters of  $\sim 100\text{-}300 \mu\text{m}$  produce the strongest signatures in UARS MLS radiances [Wu *et al.* 2004]. Scattering of such particles occurs in the Rayleigh regime for MLS frequencies  $\leq 640$  GHz. From our calculations summarized in Table 1, a 20% uncertainty in the imaginary part of permittivity for an ice particle in that size range will result in  $\sim 1\text{-}10\%$  errors in both the Mie extinction coefficients and the single scattering albedos at typical MLS measurement frequencies. For the 640 GHz, the error is about 1% or less, which is the best for the cloud measurement in the TTL [Wu and Jiang, 2004]. Uncertainties in the real part of permittivity will result larger error, e.g. a 5% error will result  $\sim 1\text{-}10\%$  in typical MLS frequencies. Fortunately, the measured value for the real part of ice permittivity is more certain at the MLS frequency range.

Typical MLS Radiometers	T (°C)	$\epsilon'$	$\epsilon''$	$\xi_e$	$ \Delta\xi_e $	$ \Delta\xi_e/\xi_e $	$ \Delta\xi_e $	$ \Delta\xi_e/\xi_e $	$\omega_0$	$ \Delta\omega_0 $	$ \Delta\omega_0/\omega_0 $	$ \Delta\omega_0 $	$ \Delta\omega_0/\omega_0 $
					( $\Delta\epsilon''=5\%$ )	( $\Delta\epsilon''=5\%$ )	( $\Delta\epsilon''=20\%$ )	( $\Delta\epsilon''=20\%$ )		( $\Delta\epsilon'=5\%$ )	( $\Delta\epsilon'=5\%$ )	( $\Delta\epsilon'=20\%$ )	( $\Delta\epsilon'=20\%$ )
63 GHz	-15	3.15	0.0042	0.000397	.0000027	0.7%	.00005	12.9%	0.356	0.033	9.3%	0.041	11.4%
	-30		0.0033	0.000342	.0000005	0.1%	.00004	11.7%	0.414	0.035	8.4%	0.043	10.5%
	-60		0.0024	0.000287	.0000036	1.3%	.00003	10.1%	0.493	0.035	7.1%	0.045	9.2%
118 GHz	-15	3.15	0.0079	0.00269	0.00010	3.7%	0.0002	6.9%	0.654	0.031	4.7%	0.042	6.5%
	-30		0.0062	0.00249	0.00011	4.5%	0.0001	5.9%	0.707	0.028	4.0%	0.039	5.5%
	-60		0.0045	0.00229	0.00012	5.3%	0.0001	4.6%	0.768	0.024	3.1%	0.034	4.4%
190 GHz	-15	3.15	0.0128	0.0147	0.00095	6.4%	0.0005	3.5%	0.822	0.019	2.4%	0.028	3.4%
	-30		0.0100	0.0142	0.00096	6.9%	0.0004	2.9%	0.855	0.016	1.9%	0.024	2.8%
	-60		0.0073	0.0136	0.00100	7.4%	0.0003	2.2%	0.890	0.013	1.4%	0.019	2.2%
203 GHz	-15	3.15	0.0137	0.0189	0.00127	6.7%	0.0006	3.4%	0.839	0.018	2.1%	0.026	3.1%
	-30		0.0107	0.0183	0.00131	7.2%	0.0005	2.6%	0.869	0.015	1.7%	0.022	2.5%
	-60		0.0078	0.0176	0.00134	7.6%	0.0003	2.0%	0.901	0.012	1.3%	0.017	1.9%
240 GHz	-15	3.15	0.0162	0.0359	0.00268	7.5%	0.0009	2.5%	0.875	0.014	1.6%	0.021	2.4%
	-30		0.0127	0.0350	0.00273	7.8%	0.0007	2.0%	0.899	0.011	1.3%	0.018	2.0%
	-60		0.0093	0.0340	0.00277	8.1%	0.0005	1.5%	0.924	0.009	1.0%	0.014	1.5%
640 GHz	-15	3.15	0.0458	1.413	0.19014	13.5%	0.0101	0.7%	0.945	0.004	0.4%	0.010	1.1%
	-30		0.0366	1.403	0.19027	13.6%	0.0081	0.6%	0.956	0.003	0.4%	0.008	0.9%
	-60		0.0274	1.392	0.19039	13.7%	0.0061	0.4%	0.967	0.002	0.2%	0.006	0.7%
2500 GHz	-15	3.15	0.4906	2.380	0.07139	3.0%	0.0439	1.8%	0.470	0.021	4.4%	0.012	2.6%
	-30		0.4544	2.353	0.08254	3.5%	0.0448	1.9%	0.481	0.022	4.8%	0.016	3.3%
	-60		0.4187	2.323	0.09618	4.1%	0.0452	1.9%	0.495	0.025	5.0%	0.020	4.0%

**Table 1:** For each typical UARS and EOS MLS radiometer frequency, this table lists the Mie efficiency coefficient, single scattering albedo for a typical ice particle of 200  $\mu\text{m}$  in diameter at three different temperatures ( $-15^\circ\text{C}$ ,  $-30^\circ\text{C}$  and  $-60^\circ\text{C}$ ), and their percentage errors resulted from 20% uncertainty in imaginary part of ice permittivity (blue) or 5% uncertainty in real part of ice permittivity (green).

## 5. Summary

The empirical model of dielectric ice permittivity is extended to frequencies as high as 4 THz from the previous LH formulae. The modified LH model may have uncertainties about

12% in imaginary part and 5% in the real part of ice permittivity at frequency range of 1-1000 GHz in comparisons with laboratory data. At higher frequencies (>1000GHz) the uncertainties may be up to ~50% in imaginary part and ~15% in real part, respectively. For liquid water, uncertainties are 5% or less in both imaginary and real parts of the permittivity for temperature  $\leq 0^{\circ}\text{C}$ . Additional uncertainties may exist at lower temperatures where little laboratory measurements are available.

Such uncertainties in ice and water permittivity may result in about 10-20% in combined errors in the Mie theory calculations. Thus more lab measurements are needed to improve our knowledge of permittivity. Also, our empirical model is based only on pure ice and liquid water. Impurity effects on ice permittivity are little known, such as those formed in polar stratospheric clouds (PSCs). Although this study is primarily motivated by the current MLS cloud studies, it also has important applications to other ground, airborne, space microwave sensors.

## Acknowledgements

The authors wish to express their gratitude to Paul Wagner and Joe Waters for helpful comments and suggestions. This work was conducted at the Jet Propulsion Laboratory, California Institute of Technology, under contract with the National Aeronautics and Space Administration.

## References

- Cumming, W.A., The dielectric properties of ice and snow at 3.2 centimeters, *J. Appl. Phys.*, 23, 768-773, 1952.
- Bertie, J.E., H.J. Labbe, and E. Whalley, Absorptivity of Ice I in the Range 4000-30  $\text{cm}^{-1}$ , *J. Chem. Phys.*, 50, 4501-4520, 1969.
- Hufford, G., A model for the complex permittivity of ice at frequencies below 1 THz. *Int. J. Infrared Millimeter Waves*, 12, 677-682, 1991.
- von Hippel, A. (ed), *Dielectric Materials and Applications*, MIT Press, Cambridge, MA, 1945.
- von de Hulst, H. C., *Light Scattering by Small Particles*. pp 470, New York, Dover, 1981.
- Jiang, J.H, B. Wang, K. Goya, K. Hocke, S.D. Eckerman, J. Ma, D.L. Wu, W.G. Read, "Geographical Distribution and Inter-Seasonal Variability of Tropical Deep Convection: UARS MLS Observations and Analyses," *J. Geophys. Res.* 109, D3, D03111, 10.1029/2003JD003756,2004.
- Klein, L.A., and C.T. Swift, An Improved Model for the Dielectric Constant of Sea Water at Microwave Frequencies, *IEEE Transactions on Antennas and Propagation*, Vol. 25, 1977.
- Lamb, J., Measurements of the Dielectric Properties of Ice, *Discuss. Faraday Soc.*, 42A, p238, 1946.
- Lamb, J., and A. Turney, The dielectric properties of ice at 1.25 cm. wavelength, *Proc. Phys. Soc. London Sect.*, B 62, 272-273, 1949.
- Liebe, H. J., T. Manabe, and G. A. Hufford, Millimeter-wave attenuation and delay rates due to fog/cloud conditions. *IEEE Trans. Ant. Prop.*, 37, 1617-1623, 1989.
- Liebe, H. J., G. A. Hufford, and T. Manabe, A model for the complex permittivity of water at frequencies below 1 THz, *Int. J. Infrared and Millimeter Waves*, 12-7, 659-674, 1991.
- Lowan, A.N., Tables of Scattering Functions for Spherical Particles, U.S. National Bureau of Standards, *Applied Mathematics Series* 4, 1949.
- Matzler, C., and U. Wegmuller, Dielectric properties of freshwater ice at microwave frequencies, *J. Phys. D: Appl. Phys.*, 20, 1623-1630, 1987.
- Mishima, O., D. D. Klug, and E. Whalley, The far-infrared spectrum of ice Ih in the range 8-25 $\text{cm}^{-1}$ . Sound waves and difference bands, with application to Saturn's rings. *J. Chem. Phys.*, 78, 6399-6404, 1983.
- Perry, J., and A.W. Straiton, Revision of dielectric-constant of ice in millimeter-wave spectrum, *J. Appl. Phys.*, 44(11), 5180-5180, 1973.
- Read, W.G., D.L. Wu, J.W. Waters, H.C. Pumphrey, "Dehydration in the Tropical Tropopause Layer: Implications from UARS MLS," *J. Geophys. Res.*, in press.
- Whalley, E., and H.J. Labbe, Optical Spectra of Orientationally Disordered Crystals. III. Infrared Spectra of the

- Sound Waves, *J. Chem. Phys.*, **51**, 3120-3127, 1969.
- Ulaby, F. T., Moore, R. K., and Fung, A. K., *Microwave Remote Sensing: Active and Passive, Volume I: Microwave Remote Sensing Fundamentals and Radiometry*, Artech House, Inc., 1981.
- Vant, M.R., R.B. Gray, R.O. Ramseier, and V. Makios, *J. Appl. Phys.*, 45, p4712, 1974.
- Wu, D.L., W.G. Read, A.E. Dessler, S.C. Sherwood, J.W. Waters, "UARS MLS Cloud Ice Measurements and Implications for H<sub>2</sub>O Transport near the Tropopause," *J. Atmos. Sci.*, in review.
- Wu, D. L., and J. H. Jiang, EOS MLS Algorithm Theoretical Basis for Cloud Measurements, *Technical Report*, Jet Propulsion Laboratory, D-19299, EOS MLS DRL 601, ATBD-MLS, 2004.